Investigation of Doppler broadening Compton scattering for aluminum element at different angles

Wrood K. Abood, Mahdi H. Jasim

Department of Physics, College of Science, University of Baghdad, Baghdad, Iraq

E-mail: wrood_k@yahoo.com

Abstract

The Compton energy-absorption cross sections are evaluated for the Al element and for a photon energy range (1 - 100 keV). By using these cross-sections, the Compton component of the mass–energy absorption coefficient is derived, where the electron momentum prior to the scattering event caused a Doppler broadening of the Compton line. Also, the momentum resolution function is evaluated in terms of incident and scattered photon energy and scattering angle. The overall momentum resolution of each contribution is estimated for X-ray and γ-ray energies of experimental interest in the angular region 30°–180° and the best angle is found at the scattering angle 180°. The Compton broadening is estimated using the nonrelativistic formula in the presence of these angular regions, for the photon energy range (17.44 – 68.81) keV. The measured cross sections are compared with theoretical values and reported values of other investigators. The present results agree with the theoretical values.

Key words

Doppler broadening, Compton profile, cross section.

Article info.

Received: Jun. 2015
Accepted: Sep. 2015
Published: Dec. 2015

دراسة توسيع دوبلر لاستطارة كومبتون لعنصر الالمنيوم عند زوايا مختلفة

ورود كريم عبود، مهدي هادي جاسم

قسم الفيزياء، كلية العلوم، جامعة بغداد، بغداد، العراق

الخلاصة

تم ايجاد المقاطع العرضية لامتصاص طاقة كومبتون لعنصر Al ولمدى طاقة الفوتون بين 1-100 ك.أ.ف. وباستخدام هذه المقاطع العرضية اشتقت مركبة كومبتون لمعامل الامتصاص الكتلة - الطاقة، حيث ان زخم الالكترون قبيل حدوث التشتت سبب في ظهور توسع دوبلر في خط كومبتون. تم ايجاد قيم دالة ميز الزخم بدلالة طاقة الفوتون الساقط والمشتت وزاوية التشتت. قدرميز الزخم الاجمالي لكل مساهمة من الطاقات العملية ذات الاهتمام للأشعة السينية و اشعة كاما وعند مدى الزوايا 30°–180° وافضل زاوية استطارة كانت 180°m. كذلك تم تحديد توسع كومبتون باستخدام الصيغة غير النسبية لهذا والمدى طاقة الفوتون(17.44-68.81) ك.أ.ف. قورنت نتائج المقاطع العرضية المقاسة مع القيم النظرية والمعلنة لباحثين اخرين. وجد ان النتائج الحالية تتوافق مع القيم النظرية.

Introduction

Compton effect is a scattering of gamma or X-rays by a charged particle in which a portion of its energy is given to the charged particle inelastic collision. The major physical effects characterizing the backward-scattered spectra are besides attenuation, Compton shift and material-specific Doppler broadening of the photon spectrum in the sample. The shape of a Compton-broadened peak can reveal information about the electron momentum of an elementary or, even to some extent, of a chemical compound. Essentially, two

types of methods were considered for describing the broadening of the characteristic lines. The first calculation procedure evaluated scattered spectra based on tabulated material specific Compton profiles. The second model was a phenomenological approach, it fitted a function consisting of Gaussian curves above a linearly approximated background to the curvature of the 2nd derivative of the Compton spectrum. These methods were experimentally validated on Compton profiles of a variety of sample materials containing period 2 and period 3 elements [1].

It was proven that, in principle, a comparing of measured spectra with calculated spectra provides high material differentiation capabilities, but for most molecules tabulated Compton profiles are not available and the independent atom approximation causes deviations. The phenomenological method was employed to extract Gaussian curve fit-parameters to distinguish measured materials quantitatively. Most of the samples could be distinguished from each other based on their profile structure [1].

Compton energy absorption cross-sections are calculated using the formulas based on a relativistic impulse approximation (in which a particle's path is assumed to be a straight line right through the scattering region) to assess the contribution of Doppler broadening and to examine the Compton profile literature and explore what, if any, effect our knowledge of this line broadening has on the Compton component in terms of mass–energy absorption coefficient. The electron momentum prior to the scattering event should cause a Doppler broadening of the Compton line [1]. Measurement of differential scattering cross sections for X-rays is useful in the studies of radiation attenuation, transport and energy deposition and plays an important role in medical physics, reactor shielding, industrial radiography in addition to X-ray crystallography. Coherent (Rayleigh) scattering accounts for only a small fraction of the total cross section, contributing at the most to 10% in heavy elements, just below the K-edge energy. Incoherent (Compton) scattering accounts for the rest of the total cross section. For low Z materials, this process dominates over most part of the energy range. The Compton profile provides detailed information about the electron momentum distribution in the scatterer. This technique is particularly sensitive to the behavior of the slower moving outer electrons involved in bonding in condensed matter and can be used to test their quantum-mechanical description. Mendelsohn et al. (1974) [2] made calculations of relativistic Hartree-Fock (RHF) Compton profile $J(q)$ for the rare gases and Pb, for values of q between 0 and 100 and were compared with the non-relativistic calculations. Comparison with experimental profile data was made for Ar and Kr. For q between 0.0 and 0.4 in Kr, much closer agreement with the experiment is obtained when the relativistic HF wave function is used to perform the profile calculation than when the non-relativistic HF. Robert Benesch (1976) [3], calculated Compton profile by HF wave functions for the neutral atoms As ($Z = 33$) through Yb ($Z = 70$) and the comparison with the results of relativistic HF wave functions indicates that the overall effect of using the relativistic functions is to produce the total $J(q)$, which are flatter at the center than those computed from non-relativistic HF wave functions. Rao et al. (2002) [4] calculated the Compton energy absorption cross-sections using the formulas based on a relativistic impulse approximation to assess the contribution of Doppler broadening and to examine the Compton profile. Using these cross sections, the Compton component of the mass–energy absorption coefficient is derived in the

energy region from 1 keV to 1 MeV for all elements with Z=51 – 100. Also they estimated the Compton broadening using the non-relativistic formula in the angular region 1°–180°, for 17.44, 22.1, 58.83, and 60 keV photons for few elements (H, C, N, O, P, S, K, and Ca). Rao et al. (2004) [5] used relativistic and non-relativistic Compton profile cross sections for H, C, N, O, P, and Ca and for a few important biological materials such as water, polyethylene, polystyrene, nylon, polycarbonate, Bakelite, fat, bone and calcium hydroxyapatite that estimated, for X-ray and ^{241}Am (59.54 keV) photons energies. These values are estimated around the centroid of the Compton profile with an energy interval of 0.1 and 1.0 keV for 59.54 keV photons. P. Singh (2011) [6] studied the Compton scattering differential cross-sections for the 19.648 keV photons in a few elements with $6 \leq Z \leq 50$. The measured Compton scattering cross-sections are compared with the theoretical Klein-Nishina cross-sections corrected for the non-relativistic HF incoherent scattering function S(X, Z). Hossain et al. (2012)[7] studied Compton scattering using NI (Tl) scintillator detector and a collimated ^{137}Cs source producing gamma rays with an energy of 662keV scattered incoherently by Al and Cu materials through the angles from 0 to 120°. The Compton scattering effect is investigated and found that the energy of the scattered gamma ray decreases as the scattering angle increases. The differential scattering cross-section as a function of scattering angles is also measured. The experimental results of differential scattering cross-sections for Al and Cu materials were compared with a function of a scattering angle and found to coincide at the higher angle region, although scattering cross-sections for Cu are larger than Al scatter at the lower angles region.

In the present work, a proposal for calculating Compton profile required for the calculations of Doppler broadening and double differential cross- section. These calculations are presented and tested of Al element. the Compton profile can be determined from measurements of the partial differential cross section by performing a constant energy scan at the scattering angles (30^o, 45^o, 60^o, 90^o, 180^o).

Theory

The differential cross section for the scattering of gamma photons with free electrons was first derived in 1928 by Oskar Klein and Yoshio Nishina [8] using the quantum electrodynamics approach. The angular distribution of the scattered photon is known as the Klein-Nishina cross-section formula [9] and given by:

$$\frac{d\sigma}{d\Omega} = \frac{Zr_\circ^2}{2}\left(\frac{1+cos^2\theta}{\left(1+\alpha(1-cos\theta)\right)^2}\right)\left(1+\frac{\alpha^2(1-cos\theta)^2}{(1+cos^2\theta)[1+\alpha(1-cos\theta)]}\right) \quad (1)$$

where $\alpha = \frac{E_\gamma}{mc^2}$which is the energy of the photon in the units of the electrons rest mass and $r_\circ$ is the classical electron radius $r_e = \frac{e^2}{4\pi\varepsilon_0 m_e c^2} = 2.817 \times 10^{-15} m$. However, what has been stated earlier is valid assuming that the gamma interacts with an electron at rest. But this is an approximation. If the electron momentum is taken into account, neither the angle-energy relations nor the Klein-Nishina formula, Eq. (1) are completely valid. The electron pre-collision momentum creates a broadening in the energy spectrum of the scattered photon which is known as the Doppler broadening effect [10]. The distance travelled by the electron ejected from

the atom is shorter than the spatial resolution of today's solid state detectors, making it impossible to measure the energy and momentum of the electron in order to correct this effect. This effectively introduces an error on the calculated Compton scattering angle θ. The angular Klein-Nishina is integrated to give the total cross section for a given energy which is given as[11]:

$$\sigma_{KN} = 2\pi r_{\circ}^2 \left\{\frac{1+\alpha}{\alpha^2}\left[\frac{2(1+\alpha)}{1+2\alpha} - \frac{1}{\alpha}\ln(1+2\alpha)\right] + \frac{1}{2\alpha}\ln(1+2\alpha) - \frac{1+3\alpha}{(1+2\alpha)^2}\right\} \quad (2)$$

The Doppler broadening effect imposes an inherent limitation on the angular resolution. In general, the interaction takes place with a bound, moving electron. The momentum of the electron results in a broadening of the gamma spectrum lines and this leads to an error on the computation of the Compton scattering angle. The equation that accounts for the electron movement is[12]

$$P_z = -mc\frac{E_\gamma + E_\gamma^{'} - E_\gamma E_\gamma^{'}\frac{1-cos\theta}{mc^2}}{\sqrt{(E_\gamma)^2 + (E_\gamma^{'})^2 - 2\,E_\gamma E_\gamma^{'}\,cos\theta}} \quad (3)$$

where p_z is the electron momentum, before the interaction, projected upon the gamma momentum transfer vector and$E_\gamma^{'}$ is the gamma photon energy immediately after the interaction. This equation reduces exactly to Eq. (3) taking p_z= 0. The angular distribution is also affected by the electron motion and the Klein-Nishina cross-section must be modified giving the following expression[13]:

$$\frac{d^2\sigma}{d\Omega dE_\gamma^{'}} = \frac{mr_{\circ}^2}{2E_\gamma}\left(\frac{E^{'}}{E_\gamma} + \frac{E_\gamma}{E^{'}} - sin^2\theta\right)\frac{E_\gamma^{'}}{\sqrt{(E_\gamma)^2 + (E_\gamma^{'})^2 - 2\,E_\gamma E_\gamma^{'}\,cos\theta}}J(p_z) \quad (4)$$

where E_γ is the Compton energy calculated from θ through Eq. (3), and *J(p_z)*, known as Compton profile which is the electron momentum distribution on the material. The values of the Compton profiles are important as they give insight of the electron movement in the atom. They have been calculated using the HF method [14 , 15]. *J(p_z)* and $J_{mag}(pz)$are the Compton and magnetic Compton profiles which are properties of the scattering electrons. They are defined as the one-dimensional projections of the electron and spin momentum density distributions, respectively. By including the normalizing pre factors 1/N and 1/μ, where N and μ represent the total number of electrons and the spin-unpaired electrons only, we choose the integrated profile areas to be equal to the total charge and spin of the system. Thus,

$$J(pz) = {}^1/_N \iint_{-\infty}^{\infty} n(p)dp_x dp_y \quad (5)$$

In an Spherically Symmetric system the expression is commonly rewritten in terms of the radial momentum distribution *I (**p**)* = 4πp^{2}n(***p***) and a scalar momentum variable, *q,* as

$$J_{mag}(pz) = {}^1/_\mu \iint_{-\infty}^{\infty}(n\uparrow(p) - n\downarrow(p))dp_x dp_y \quad (6)$$

where n(p), n↑ (p) and n↓ (p) are the three-dimensional electron momentum distributions for all, majority-spin (↑) and minority-spin (↓) electrons, respectively. The Compton profile is therefore the one dimensional projection

of the nuclear momentum distribution along the direction of q. The Compton profile can be determined from measurements of the partial differential cross section by performing a constant energy scan through all possible scattering angles.

Apparatus

The gamma detector used in the present work is (3"× 3") NaI (Tl) scintillation detector. The system is portable and can be used in the laboratories and field work. It has a fully-integrated multi-channel analyzer (MCA) tube base that contains a high-voltage power supply and pre amplifier; all supplied by Canberra industries USA. The source is cylindrical ^{137}Cs of 0.8 cm in the diameter activity was 8 mCi giving collimated gamma rays at the exit of the lead collimator of the same dimension. Samples are located at 15 cm after the radioactive source and the measurement time was 15 minutes. The experimental, arrangement of the measurements is shown schematically in Fig. 1.

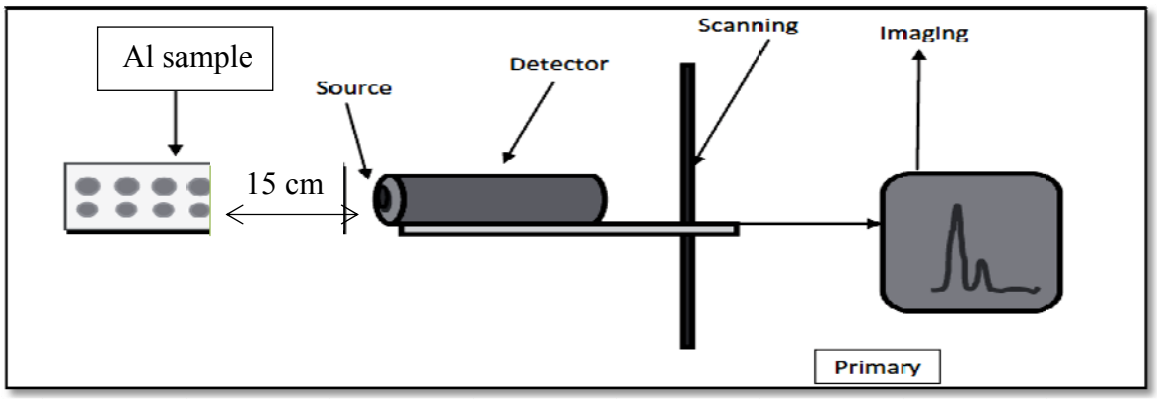

Fig. 1: Experimental setup for plate imaging with the source in direct contact with the detector and depressions toward the source [16].

Results and discussion

We calculated the Compton profile theoretically by equalizing through program table curve, 2D soft ware", version 5.01 program. The best estimated theoretical equation was given by

$$J^{-1} = A + B\,Q^{1.5} \qquad (7)$$

where J (Compton profile) and Q (average electron momentum in the ground state of hydrogen). When the parameters (A and B) for these test power intensities are calculated for J and Q value

$A = 0.5775\ Z^{-0.402}$

and

$B = 7.4473\ Z^{-1.238}$ (8)

The predicted A and B coefficient is an archived from fitting to the experimental result, Z is atomic number and theoretical calculation of the Compton profile (J and Q),where the best –fit linear regression line is a curved at $r^2 = 1$.

The Doppler broadening is calculated by using Eq. (3), and the Tables from 1 to 5 show the degree of Doppler broadening in a target atom which can be calculated from the probability for Compton scattering from an electron in nth sub-shell into a scatter energy and scatter angle of E_A and E_0, respectively. In the present study, different angles are taken $(30^\circ, 45^\circ, 60^\circ, 90^\circ, 180^\circ)$ for *Al* sample to calculate the Compton profile and the double-differential scattering cross section of Doppler broadening

(DDSCS), the best angle is found at the scattering angle 180°, it is scattered in the backward direction inside a narrow cone with the axis that coincides with the incoming electron beam. The electron momentum prior to the scattering event should cause a Doppler broadening of the Compton line. The momentum resolution function is evaluated in terms of an incident and scattered photon energy and scattering angle. The overall momentum resolution of each contribution is estimated for X-ray and γ-ray energies an experimental interest angular region 30°–180°. The Compton broadening is also, estimated using the non-relativistic and relativistic formulae for photon energies 17.44, 22.1, 58.83, and 68.18keV, respectively.

Table 1: The double-differential scattering cross section of Doppler broadening at angle 30° for Al.

E_0(keV)	E_A(keV)	E_C(keV)	Q= E_C/13.6	A	B	J $(\frac{\hbar}{mc^2})^{-1}$	J $(\frac{\hbar}{mc^2})$	$\frac{d^2\sigma}{d\Omega dE_A}$	Q Theo [14]	J$(\frac{\hbar}{mc^2})$ Theo[14]
17.44	16.95072	0.489277	0.035976	0.205943	0.310947	0.208065	4.806197	1.08169E-48	0	5.15E+00
22.1	21.32016	0.779836	0.057341	0.205943	0.310947	0.210212	4.757093	1.07917E-48	0.05	5.11E+00
23.1	22.24935	0.850648	0.062548	0.205943	0.310947	0.210807	4.743676	1.07797E-48	0.1	5.00E+00
24.1	23.17558	0.924417	0.067972	0.205943	0.310947	0.211453	4.729178	1.07652E-48	0.15	4.82E+00
24.2	23.26804	0.931956	0.068526	0.205943	0.310947	0.211521	4.727668	1.07636E-48	0.2	4.57E+00
25.2	24.19104	1.008963	0.074188	0.205943	0.310947	0.212226	4.711953	1.07462E-48	0.3	3.37E+00
30.85	29.35134	1.498661	0.110196	0.205943	0.310947	0.217317	4.601565	1.05968E-48	0.4	3.32E+00
32.06	30.44455	1.61545	0.118783	0.205943	0.310947	0.218673	4.573047	1.05531E-48	0.5	2.76E+00
33.36	31.61445	1.745549	0.128349	0.205943	0.310947	0.220241	4.540483	1.05014E-48	0.6	2.34E+00
34.57	32.69908	1.87092	0.137568	0.205943	0.310947	0.221809	4.508391	1.0449E-48	0.7	2.04E+00
35.86	33.8509	2.009097	0.147728	0.205943	0.310947	0.223598	4.472305	1.03885E-48	0.8	1.84E+00
39.91	37.43711	2.472888	0.18183	0.205943	0.310947	0.230052	4.34684	1.01682E-48	1	1.62E+00
42.76	39.93383	2.826175	0.207807	0.205943	0.310947	0.235399	4.248106	9.98651E-49	1.2	1.49E+00
45.72	42.50372	3.216278	0.236491	0.205943	0.310947	0.241704	4.137296	9.77623E-49	1.4	1.38E+00
48.72	45.08457	3.635428	0.267311	0.205943	0.310947	0.248917	4.017397	9.54268E-49	1.6	1.26E+00
48.81	45.16163	3.648369	0.268262	0.205943	0.310947	0.249147	4.013694	9.53538E-49	1.8	1.14E+00
52.02	47.89625	4.123749	0.303217	0.205943	0.310947	0.257861	3.878064	9.26494E-49	2	1.03E+00
58.83	53.61006	5.21994	0.383819	0.205943	0.310947	0.279882	3.572931	8.63829E-49	2.4	8.16E-01
59.54	54.19902	5.340976	0.392719	0.205943	0.310947	0.282469	3.540214	8.56985E-49	3	5.68E-01
66.24	59.69542	6.544579	0.481219	0.205943	0.310947	0.309744	3.228477	7.90767E-49	4	3.22E-01
68.18	61.26646	6.913535	0.508348	0.205943	0.310947	0.318644	3.138299	7.71305E-49	5	1.99E-01
									6	1.34E-01
									7	9.48E-02
									8	6.96E-02
									10	3.90E-02
									15	1.10E-02
									20	3.50E-03
									30	5.10E-04
									40	1.10E-04
									60	1.20E-05
									100	6.00E-07

The behavior of the Double differential cross section as function of the photon energy for *Al* sample at $\theta = 30°$ scattering angle shown in Fig.1a.

Which is the Compton profile distribution as function of the average electron momentum in the ground state of hydrogen Q is given in Fig.1b,

where the experimental empirical results an in a consistence with the theoretical results. In Q region (0.01-1).

Table 2: The double-differential scattering cross section of Doppler broadening at angle 45° for Al

E_0(keV)	E_A(keV)	E_C(keV)	Q	A	B	$J^{-1}(\frac{\hbar}{me^2})^{-1}$	$J(\frac{\hbar}{me^2})$	$\frac{d^2\sigma}{d\Omega dE_A}$	Q Theo [14]	$J(\frac{\hbar}{me^2})$ Theo[14]
17.44	17.16197	0.27803	0.020443	0.205943	0.310947	0.206852	4.83438	1.89367E-48	0	5.15E+00
22.1	21.65543	0.444567	0.032689	0.205943	0.310947	0.207781	4.812769	1.91374E-48	0.05	5.11E+00
23.1	22.61473	0.485268	0.035681	0.205943	0.310947	0.208039	4.806799	1.91318E-48	0.1	5.00E+00
24.1	23.57229	0.527712	0.038802	0.205943	0.310947	0.20832	4.800317	1.91241E-48	0.15	4.82E+00
24.2	23.66795	0.532052	0.039121	0.205943	0.310947	0.208349	4.79964	1.91232E-48	0.2	4.57E+00
25.2	24.62359	0.576408	0.042383	0.205943	0.310947	0.208656	4.792577	1.91132E-48	0.3	3.37E+00
30.85	29.99056	0.859445	0.063194	0.205943	0.310947	0.210883	4.741975	1.90133E-48	0.4	3.32E+00
32.06	31.13283	0.927172	0.068174	0.205943	0.310947	0.211478	4.728627	1.89817E-48	0.5	2.76E+00
33.36	32.35729	1.002712	0.073729	0.205943	0.310947	0.212168	4.713248	1.89434E-48	0.6	2.34E+00
34.57	33.4944	1.075598	0.079088	0.205943	0.310947	0.212859	4.697949	1.89038E-48	0.7	2.04E+00
35.86	34.70397	1.156026	0.085002	0.205943	0.310947	0.213649	4.680577	1.88571E-48	0.8	1.84E+00
39.91	38.4833	1.426699	0.104904	0.205943	0.310947	0.216508	4.618766	1.86804E-48	1	1.62E+00
42.76	41.12643	1.633567	0.120115	0.205943	0.310947	0.218887	4.568561	1.85279E-48	1.2	1.49E+00
45.72	43.85737	1.862632	0.136958	0.205943	0.310947	0.221703	4.510533	1.83447E-48	1.4	1.38E+00
48.72	46.61055	2.109452	0.155107	0.205943	0.310947	0.224938	4.445678	1.81332E-48	1.6	1.26E+00
48.81	46.69292	2.117084	0.155668	0.205943	0.310947	0.225041	4.44364	1.81265E-48	1.8	1.14E+00
52.02	49.62214	2.397861	0.176313	0.205943	0.310947	0.228963	4.367512	1.78712E-48	2	1.03E+00
58.83	55.78163	3.048374	0.224145	0.205943	0.310947	0.23894	4.185146	1.72381E-48	2.4	8.16E-01
59.54	56.41955	3.120446	0.229445	0.205943	0.310947	0.240117	4.164629	1.71654E-48	3	5.68E-01
66.24	62.4004	3.839599	0.282323	0.205943	0.310947	0.252588	3.959016	1.64243E-48	4	3.22E-01
68.18	64.1191	4.060903	0.298596	0.205943	0.310947	0.256678	3.895927	1.61931E-48	5	1.99E-01
									6	1.34E-01
									7	9.48E-02
									8	6.96E-02
									10	3.90E-02
									15	1.10E-02
									20	3.50E-03
									30	5.10E-04
									40	1.10E-04
									60	1.20E-05
									100	6.00E-07

Similar calculations have been done for the DDSCS of the Doppler broadening at the scattering angles 45°, 60°, 90°, 180°. The results are given in Tables (2-5) and plotted against energy Figs. (2a)-(5a). Also comparison between the theoretical and empirical as function of the average electron momentum in the ground state of hydrogen Q values of Compton profile for each angle are sketched in plots given in Figs.(2b)-

(5b). The distribution as a function of the, when the experimental empirical results an in a consistence with the theoretical [13].

Table 3: The double-differential scattering cross section of Doppler broadening at angle 60° for Al.

E_0(keV)	E_A(keV)	E_C(keV)	Q	A	B	$J^{-1}(\frac{\hbar}{me^2})^{-1}$	$J(\frac{\hbar}{me^2})$	$\frac{d^2\sigma}{d\Omega dE_A}$	Q Theo [14]	$J(\frac{\hbar}{me^2})$ Theo[14]
17.44	16.3505	1.089503	0.08011	0.205943	0.310947	0.212993	4.694982	4.75273E-49	0	5.15E+00
22.1	20.3792	1.720799	0.126529	0.205943	0.310947	0.219938	4.546738	4.68646E-49	0.05	5.11E+00
23.1	21.22655	1.87345	0.137754	0.205943	0.310947	0.221841	4.507737	4.66437E-49	0.1	5.00E+00
24.1	22.06797	2.03203	0.149414	0.205943	0.310947	0.223901	4.46625	4.63949E-49	0.15	4.82E+00
24.2	22.15179	2.048212	0.150604	0.205943	0.310947	0.224116	4.461966	4.63685E-49	0.2	4.57E+00
25.2	22.98676	2.213243	0.162738	0.205943	0.310947	0.226357	4.417809	4.60892E-49	0.3	3.37E+00
30.85	27.59711	3.252891	0.239183	0.205943	0.310947	0.242316	4.126841	4.40179E-49	0.4	3.32E+00
32.06	28.5614	3.498596	0.25725	0.205943	0.310947	0.246514	4.056562	4.34748E-49	0.5	2.76E+00
33.36	29.58861	3.77139	0.277308	0.205943	0.310947	0.251351	3.978506	4.28571E-49	0.6	2.34E+00
34.57	30.5366	4.033396	0.296573	0.205943	0.310947	0.256164	3.903753	4.22529E-49	0.7	2.04E+00
35.86	31.53878	4.321216	0.317736	0.205943	0.310947	0.261634	3.822132	4.15805E-49	0.8	1.84E+00
39.91	34.62946	5.280539	0.388275	0.205943	0.310947	0.281174	3.556522	3.9315E-49	1	1.62E+00
42.76	36.7551	6.004904	0.441537	0.205943	0.310947	0.297173	3.365047	3.762E-49	1.2	1.49E+00
45.72	38.92105	6.798946	0.499923	0.205943	0.310947	0.315854	3.166024	3.5812E-49	1.4	1.38E+00
48.72	41.07414	7.645863	0.562196	0.205943	0.310947	0.337017	2.967208	3.39638E-49	1.6	1.26E+00
48.81	41.13809	7.671913	0.564111	0.205943	0.310947	0.337688	2.961317	3.39085E-49	1.8	1.14E+00
52.02	43.39497	8.625029	0.634193	0.205943	0.310947	0.362986	2.754928	3.19481E-49	2	1.03E+00
58.83	48.03328	10.79672	0.793877	0.205943	0.310947	0.425889	2.348032	2.79711E-49	2.4	8.16E-01
59.54	48.50554	11.03446	0.811357	0.205943	0.310947	0.433193	2.30844	2.75765E-49	3	5.68E-01
66.24	52.86142	13.37858	0.983719	0.205943	0.310947	0.509327	1.963376	2.40797E-49	4	3.22E-01
68.18	54.08965	14.09035	1.036055	0.205943	0.310947	0.533857	1.873159	2.31483E-49	5	1.99E-01
									6	1.34E-01
									7	9.48E-02
									8	6.96E-02
									10	3.90E-02
									15	1.10E-02
									20	3.50E-03
									30	5.10E-04
									40	1.10E-04
									60	1.20E-05
									100	6.00E-07

Table 4: The double-differential scattering cross section of Doppler broadening at angle 90° for Al.

E_0 (keV)	E_A(keV)	E_C(keV)	Q	A	B	$J^{-1}(\frac{\hbar}{me^2})^{-1}$	$J(\frac{\hbar}{me^2})$	$\frac{d^2\sigma}{d\Omega dE_A}$	Q Theo [14]	$J(\frac{\hbar}{me^2})$ Theo[14]
17.44	16.61868	0.821321	0.060391	0.205943	0.310947	0.210558	4.749294	6.24744E-49	0	5.15E+00
22.1	20.79751	1.302487	0.095771	0.205943	0.310947	0.215159	4.647731	6.16554E-49	0.05	5.11E+00
23.1	21.68076	1.419241	0.104356	0.205943	0.310947	0.216425	4.620532	6.14077E-49	0.1	5.00E+00
24.1	22.55932	1.540681	0.113285	0.205943	0.310947	0.217799	4.591387	6.11338E-49	0.15	4.82E+00
24.2	22.64692	1.553081	0.114197	0.205943	0.310947	0.217943	4.588365	6.1105E-49	0.2	4.57E+00
25.2	23.52037	1.679633	0.123502	0.205943	0.310947	0.219439	4.557081	6.0802E-49	0.3	3.37E+00
30.85	28.36983	2.480171	0.182366	0.205943	0.310947	0.230159	4.344827	5.85992E-49	0.4	3.32E+00
32.06	29.38988	2.670122	0.196332	0.205943	0.310947	0.232993	4.291969	5.80231E-49	0.5	2.76E+00
33.36	30.47868	2.881323	0.211862	0.205943	0.310947	0.236265	4.232528	5.73658E-49	0.6	2.34E+00
34.57	31.48553	3.084467	0.226799	0.205943	0.310947	0.239528	4.174876	5.672E-49	0.7	2.04E+00
35.86	32.55205	3.307946	0.243231	0.205943	0.310947	0.243243	4.111108	5.59973E-49	0.8	1.84E+00
39.91	35.85491	4.055087	0.298168	0.205943	0.310947	0.256569	3.897581	5.35246E-49	1	1.62E+00
42.76	38.13861	4.621387	0.339808	0.205943	0.310947	0.267537	3.737807	5.16315E-49	1.2	1.49E+00
45.72	40.47588	5.244116	0.385597	0.205943	0.310947	0.280397	3.566378	4.95677E-49	1.4	1.38E+00
48.72	42.80958	5.910416	0.434589	0.205943	0.310947	0.295028	3.38951	4.7408E-49	1.6	1.26E+00
48.81	42.87906	5.930943	0.436099	0.205943	0.310947	0.295492	3.384181	4.73425E-49	1.8	1.14E+00
52.02	45.33671	6.683287	0.491418	0.205943	0.310947	0.313061	3.194266	4.49926E-49	2	1.03E+00
58.83	50.42373	8.406274	0.618108	0.205943	0.310947	0.357049	2.800733	4.00371E-49	2.4	8.16E-01
59.54	50.94442	8.59558	0.632028	0.205943	0.310947	0.362182	2.761041	3.95313E-49	3	5.68E-01
66.24	55.77114	10.46886	0.769769	0.205943	0.310947	0.415947	2.404154	3.49381E-49	4	3.22E-01
68.18	57.14004	11.03996	0.811761	0.205943	0.310947	0.433363	2.307535	3.36806E-49	5	1.99E-01
									6	1.34E-01
									7	9.48E-02
									8	6.96E-02
									10	3.90E-02
									15	1.10E-02
									20	3.50E-03
									30	5.10E-04
									40	1.10E-04
									60	1.20E-05
									100	6.00E-07

Table 5: The double-differential scattering cross section of Doppler broadening at angle 180° for Al.

E_0(keV)	E_A(keV)	E_C(keV)	Q	A	B	$J^{-1}(\frac{\hbar}{me^2})^{-1}$	$J(\frac{\hbar}{me^2})$	$\frac{d^2\sigma}{d\Omega dE_A}$	Q Theo [14]	$J(\frac{\hbar}{me^2})$ Theo[14]
17.44	16.5378	0.902205	0.066339	0.205943	0.310947	0.211256	4.733598	5.69146E-49	0	5.15E+00
22.1	20.67099	1.429007	0.105074	0.205943	0.310947	0.216534	4.618219	5.61318E-49	0.05	5.11E+00
23.1	21.5433	1.556701	0.114463	0.205943	0.310947	0.217985	4.587482	5.589E-49	0.1	5.00E+00
24.1	22.41053	1.689468	0.124226	0.205943	0.310947	0.219557	4.554617	5.56214E-49	0.15	4.82E+00
24.2	22.49698	1.703023	0.125222	0.205943	0.310947	0.219722	4.551214	5.55931E-49	0.2	4.57E+00
25.2	23.35868	1.841322	0.135391	0.205943	0.310947	0.221434	4.516026	5.52951E-49	0.3	3.37E+00
30.85	28.13493	2.715075	0.199638	0.205943	0.310947	0.233679	4.279369	5.31203E-49	0.4	3.32E+00
32.06	29.13785	2.922146	0.214864	0.205943	0.310947	0.236912	4.220974	5.25518E-49	0.5	2.76E+00
33.36	30.20772	3.152281	0.231785	0.205943	0.310947	0.240642	4.155555	5.19041E-49	0.6	2.34E+00
34.57	31.19646	3.373538	0.248054	0.205943	0.310947	0.244358	4.092351	5.12689E-49	0.7	2.04E+00
35.86	32.24316	3.616836	0.265944	0.205943	0.310947	0.248588	4.022718	5.05594E-49	0.8	1.84E+00
39.91	35.48052	4.429479	0.325697	0.205943	0.310947	0.26374	3.791612	4.81448E-49	1	1.62E+00
42.76	37.71529	5.044708	0.370934	0.205943	0.310947	0.276191	3.620689	4.63108E-49	1.2	1.49E+00
45.72	39.99941	5.720589	0.420632	0.205943	0.310947	0.290771	3.439135	4.43259E-49	1.4	1.38E+00
48.72	42.27695	6.443054	0.473754	0.205943	0.310947	0.307338	3.253751	4.22654E-49	1.6	1.26E+00
48.81	42.3447	6.465301	0.47539	0.205943	0.310947	0.307863	3.248196	4.22032E-49	1.8	1.14E+00
52.02	44.73977	7.280228	0.535311	0.205943	0.310947	0.327728	3.051308	3.99807E-49	2	1.03E+00
58.83	49.6864	9.143601	0.672324	0.205943	0.310947	0.37736	2.649991	3.53567E-49	2.4	8.16E-01
59.54	50.1919	9.3481	0.68736	0.205943	0.310947	0.383143	2.609995	3.48893E-49	3	5.68E-01
66.24	54.87053	11.36947	0.835991	0.205943	0.310947	0.44362	2.254179	3.06828E-49	4	3.22E-01
68.18	56.19506	11.98494	0.881246	0.205943	0.310947	0.463179	2.158993	2.95426E-49	5	1.99E-01
									6	1.34E-01
									7	9.48E-02
									8	6.96E-02
									10	3.90E-02
									15	1.10E-02
									20	3.50E-03
									30	5.10E-04
									40	1.10E-04
									60	1.20E-05
									100	6.00E-07

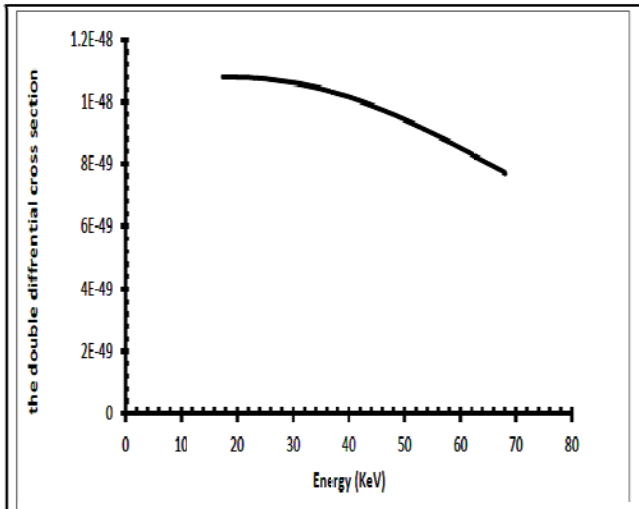

Fig. 2a: Differential coherent scattering cross sections versus photon energies at $\theta = 30^o$ for Al.

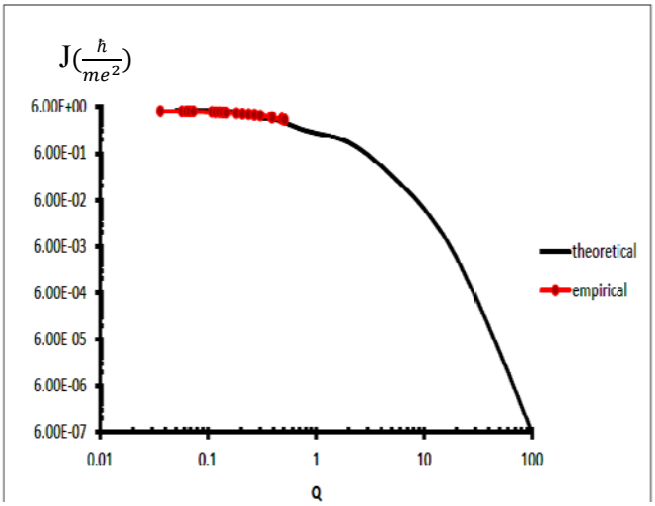

Fig. 2b: Comparison of the theoretical and empirical values for Compton profile.

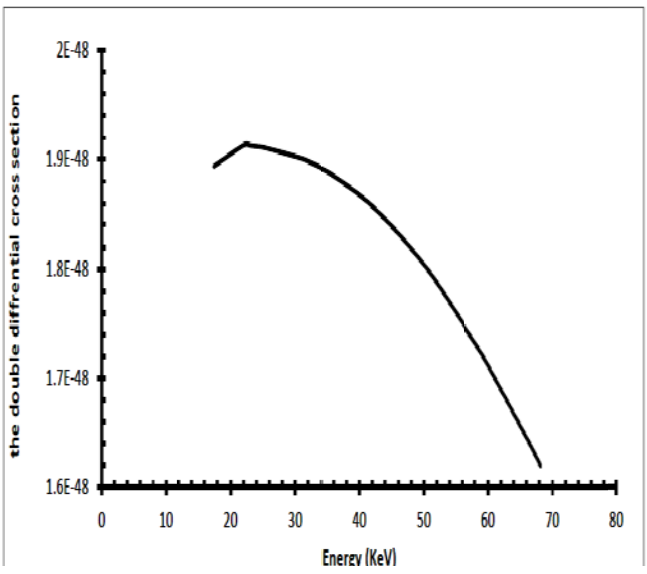

Fig. 3a: Differential coherent scattering cross sections versus photon energies at $\theta = 45^o$ for Al.

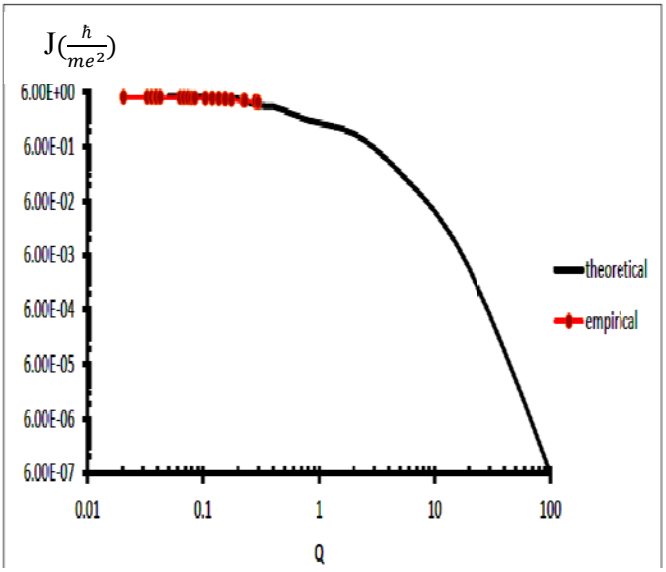

Fig. 3b: Comparison of the theoretical and empirical values for Compton profile.

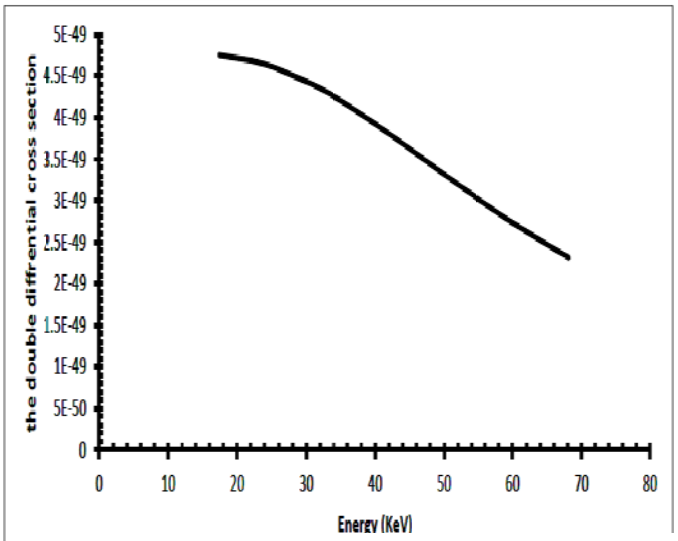

Fig. 4a: Differential coherent scattering cross sections versus photon energies at $\theta = 60^o$ for Al.

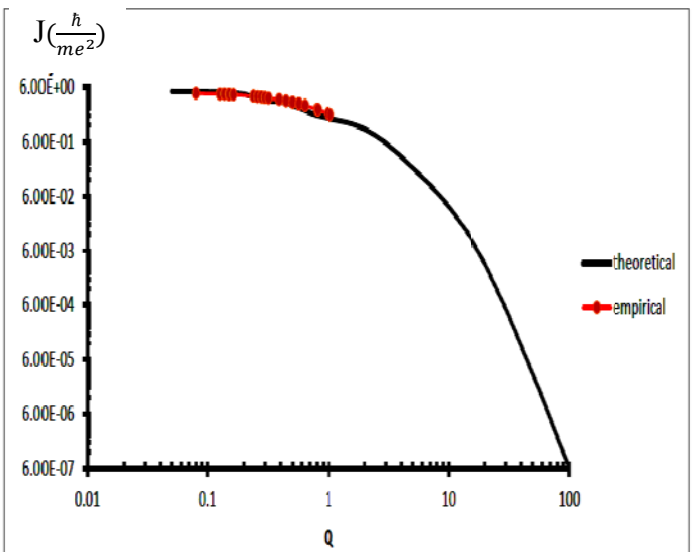

Fig. 4b: Comparison of the theoretical and empirical values for Compton profile.

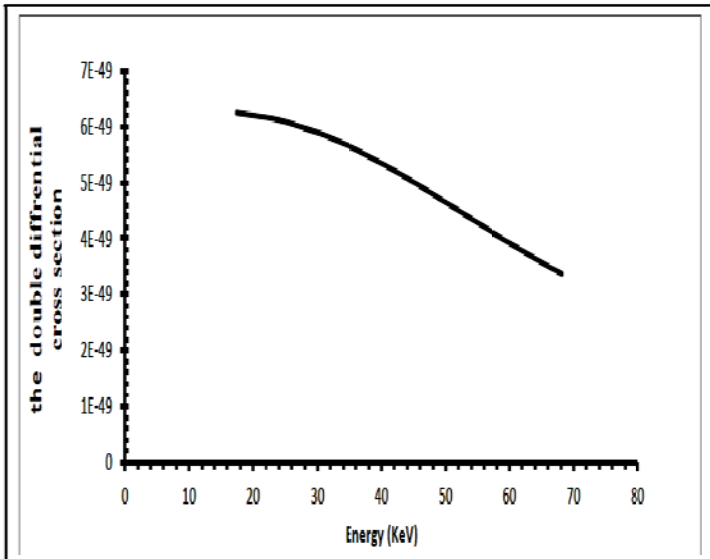

Fig. 5a: Differential coherent scattering cross sections versus photon energies at $\theta = 90^o$ for Al.

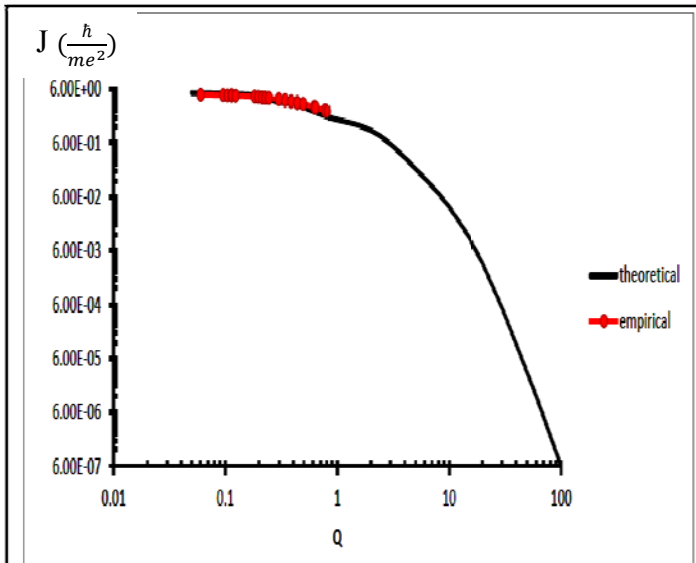

Fig. 5b: Comparison of the theoretical and empirical values for Compton profile.

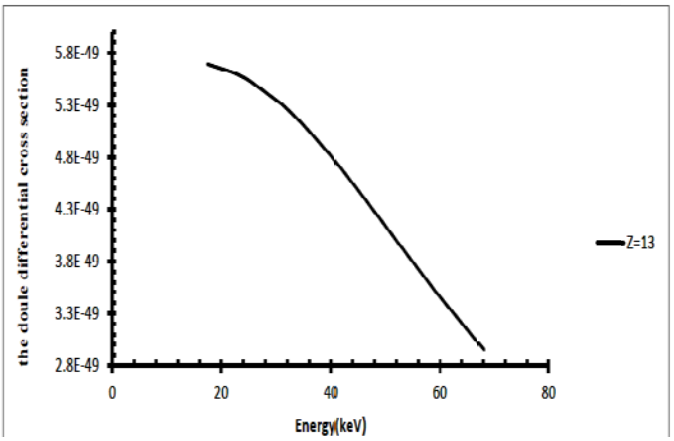

Fig. 6a: Differential coherent scattering cross sections versus photon energies at $\theta = 180^{o}$ for Al.

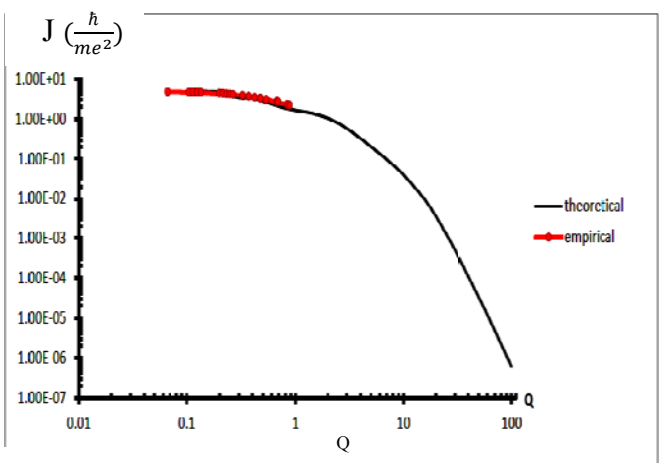

Fig. 6b: Comparison of the theoretical and empirical values for Compton profile.

Conclusions

1- The data will be useful to assess the contribution of Doppler broadening and to calculate the Compton component of the mass energy absorption coefficient.

2-The Compton profile values can be estimated from the tables and compared with the experimental results in order to know the double-differential scattering cross section of Doppler broadening.

References

[1] Malcolm J. Cooper, Rep. prog. Phys., 48 (1985) 415-481.

[2] Mendelsohn, L.B. Frank Biggs, Mann, J. B., Original Research Article Chemical Physics Letters., 26 (1974) 521-524.

[3] R.Benesch, Department of Mathematics, Roytrl Militcrty College, Kingston, Ont., CAN. J. Phys., 54 (1976) 2155-2158

[4] Rao, D. V. Takeda, b. T., and Itai, Y. and Akatsuka, T. J. Phys. Chem. Ref. Data, 31, 3 (2002) 769-818.

[5] Rao, D. Cesareo, V. R., Brunetti, A., Journal of Physical and Chemical Reference Data, 33 (2004) 627-712.

[6] Singh, P., Nature and Science Nature and Science. 9, 10 (2011) 1545-0740.

[7] Hossain, I. Azmi, N. A. Saeed, M. A. Hoque, M. E. Viswanathan, K. K., Abdullah, H. Y. International Journal of the Physical Sciences 7, 4 (2012) 544-549.

[8] Gowda S., Krishnaveni S., Yashoda T., Umesh T.K., Gowda R., J. Phys., 63 (2004) 529-541.

[9] I. Han, Demir L Nucl. Instrum. Methods, B267 (2009b) 3505-3510.

[10] Do Nascimento E, Helene O, Vanin V R, da Cruz M T F, Moralles, Nuclear Instruments and Methods in Physics Research, A 60 (2009) 244.

[11] J. Dobson, PhD. Thesis, Liverpool, (2005).

[12] C.E. Ordonez, A. Bolozdynya, W. Chang. In Nuclear Science Symposium IEEE, 2 (1997) 1361-1365.

[13] R. Ribberfors, Phys. Rev B. 12, (1975) 2067.

[14] F. Biggs, L.B. Mendelsohn, J.B. Mann. Atomic Data and Nuclear Data Tables, 16, 3 (1975) 201- 309.

[15] Y.F. Du, Z. He, G.F. Knoll, D.K. Wehe, W. Li. Evaluation of Nuclear Instruments and Methods in Physics Research Section A: Accelerators, Spectrometers, Detectors and Associated Equipment, 406, 203 (2001).

[16] Adams, F., Dams, R. "Applied Gamma-Ray Spectrometry" (1995), 2nd Edition Pergamon Pub.